Passive cooling through phase change materials in buildings. A critical study of implementation alternatives

Jesus Lizana [a]
Manuel de-Borja-Torrejon [b]
Angela Barrios-Padura [a]
Thomas Auer [b]
Ricardo Chacartegui [c]

[a] Instituto Universitario de Arquitectura y Ciencias de la Construcción, Universidad de Sevilla, Avda. Reina Mercedes 2, 41012 Seville, Spain
[b] Chair of Building Technology and Climate Responsive Design, Technical University of Munich, Arcisstrasse 21, 80333 Munich, Germany
[c] Departamento de Ingeniería Energética, Universidad de Sevilla, Camino de los Descubrimientos s/n, 41092 Seville, Spain

Abstract

Global warming is gradually increasing the cooling energy demand of buildings. Phase change materials (PCM) offer high potential to passively reduce cooling energy consumption and overheating by absorbing heat gains in the daytime through their melting process, and releasing the heat at night while solidifying by taking advantage of free cooling through natural ventilation. However, the effectiveness of PCM-based solutions highly depends on the implementation techniques, material properties, environmental conditions and occupants' behaviour. This paper analyses the performance of PCM-based solutions towards passive and low-energy cooling through a parametric study carried out in TRNSYS, in order to identify main design criteria for their optimal implementation. Two PCM implementation alternatives are assessed: a conventional passive application based on a PCM layer attached at the ceiling in contact with the indoor space, in which the heat transfer between PCM and air is based on natural convection; and an optimised low-energy application designed as a PCM layer integrated inside the suspended ceiling, in which the air flow is forced by a fan to enhance the heat transfer between PCM and the air. Both solutions are studied with and without the simultaneous operation of air-conditioning systems. A dwelling in a multi-family building was selected as a reference scenario. The results show that in the scenario with no participation of air-conditioning systems, the optimised PCM-based solution could reduce discomfort hours by 65% regarding the adaptive comfort model, and up to 83% through additional improvements in order to increase the heat transfer between PCM and air. On the other hand, the simulations reflect that both PCM-based solutions do not provide benefits in scenarios with an intermittent operation of air-conditioning systems. This study concludes with design criteria and strategies for an optimal implementation of PCM towards low-carbon buildings.

Keywords: Low-energy cooling; Low-carbon building; Passive cooling; Phase change material; Free cooling; Thermal energy storage

Nomenclature and abbreviations

AC	air-conditioning
ACH	air change rate
A_{ow}	window opening area, m^2
CDD	cooling degree-days
c_p	specific heat, KJ/kg K
CV-RMSE	coefficient of variation of the root mean square error
DH	discomfort hours, %
EC	energy consumption, kWh/m^2
h_c	convective heat transfer coefficient, W/m^2 K
HP	heat pump
H_{window}	free area height of the window
LDC	load duration curve
NMBE	normalized mean bias error
NV	night ventilation
OC	operating cost, €
PCM	phase change material
Q_v	air flow, m^3/h
R^2	coefficient of determination
t	time
T	temperature, ºC
TES	thermal energy storage
v	variant
V_{met}	meteorological wind speed at 10 m height

Greek letters

θ	air temperature, ºC
λ	thermal conductivity, W/m K
ρ	density, kg/m^3
Φ	heat gains, W

Subscript

acm	adaptive comfort model
ap	appliances
c	convection
co	comfort operative
e	outdoor
ed	daily mean
fc	forced convection
i	indoor
int	internal
l	liquid
li	lighting
oc	occupancy
rm	running mean
s	solid

1. Introduction

As a consequence of global warming, it is expected that the frequency of overheating days will increase, and that of overcooling days will decrease [1]. Such changes will affect building energy use, especially in cooling demand. Spandagos and Ng [2] assessed that future energy required by residential buildings in Hong Kong, Seoul and Tokyo, identifying an increase by 18.3-23.3%, 4-9.3% and 10.4-15.8%, respectively, over 62 years from 1983 to 2044. Huang and Hwang [1] identified an increase of energy demand in Taiwan by 31%, 59%, and 82% over current levels for the 2020s, 2050s, and 2080s. In the Mediterranean region, different studies show a significant increase of future cooling demand, with a mean cooling degree-days (CDD) trend of +4.5 (± 0.2) for 2100 [3,4]. In this context, almost 75% of building stock are considered energy inefficient [5], being more than 40% of current housing stock over 50 years old [6]. Thus, energy retrofitting of buildings through passive and low-energy cooling strategies is a priority worldwide, aimed at reducing the expected rise in energy demand [7].

The use of phase change materials through free cooling applications is a very powerful strategy for reducing the cooling demand of buildings [8]. Moreover, solutions based on latent heat storage present high thermal energy storage (TES) capacity, with low weight and compactness, which could ease energy retrofitting processes [9]. Strategies associated with phase change materials (PCMs) consist of the use of their high latent heat storage capacity throughout the phase change, from solid to fluid [10]. During the day, PCMs melt at a certain temperature while absorbing heat gains from the surrounding environment. This prevents raising air temperature in indoor spaces, contributing to maintaining thermal comfort levels. During the night, PCMs can take advantage of natural ventilation, using outdoor air at a lower temperature (free cooling) to solidify, releasing the stored heat [11]. In this application, night ventilation (NV) is crucial to discharge the absorbed heat and regenerate the storage capacity of the material [12]. Moreover, a daily temperature oscillation between 12 °C and 15 °C is required [13].

Different studies have demonstrated the viability of the constructive implementation of PCMs for passive cooling. Ramakrishnan, Wang, Sanjayan and Wilson [14] analysed the performance of building refurbishment through macro-encapsulated PCM. The results show that building refurbishment with PCM can effectively reduce the severe discomfort period (above 28ºC) by 65%, during extreme heat wave conditions, but NV is essential to release the heat absorbed throughout the day. They also concluded that the phase transition temperature and the layer thickness have a high influence on the PCM energy performance. Mi, Liu, Cui, Memon, Xing and Lo [15] studied the economic performance of 10 mm PCM layers, integrated into a lightweight wall in office buildings, in five different climate regions of China. The results show that the energy savings and economic benefits are more prominent in scenarios located in cold regions as well as in regions with hot summers and cold winters, reaching static payback periods of around 5-7 years. However, the passive cooling application of PCM did not show sufficient benefits in relatively moderate climates. Berardi and Manca [16] evaluated the implementation of PCM through passive techniques in two lightweight constructions to reduce the building cooling demand in Toronto and Vancouver. The results show that cooling demand can be reduced, depending on the climate area by 29.2%, and 59%, respectively. Sun, Zhang, Medina and Liao [17] evaluated the cooling energy reduction through a passive cooling system based on PCM integrated into Telecommunications Base Stations, identifying annual energy savings ranging from 50-67%. De Gracia [18] proposed a novel concept for passive cooling based on the dynamic use of PCM in building envelopes. The concept relies on the ability of the system to modify the position of the PCM layer inside the building envelope with respect to the insulation layer, with the aim of enhancing the solidification and melting processes of PCM. The results showed a high cooling demand reduction.

Despite the described benefits, different drawbacks limit their applications, such us material cost, low heat transfer between PCM and air, and changeable operating patterns of air-conditioning (AC) systems. The average cost of PCMs is approximately 6 €/kg, with more than 250 commercially available compounds existing, mainly based on paraffins, salt hydrates and eutectic alloys [19]. Along with the high cost, scenarios of PCM integration into building walls, floors or ceilings in contact with indoor environment, present a low heat transfer coefficient (h_c) between the air and the PCM, associated with natural convection, which limits the heat storage in the material [20]. David, Kuznik and Roux [21] compared most

common correlations to calculate convective heat transfer coefficients in a PCM wall with natural convection. They showed that even having a favourable mixed convection in both laminar and turbulent regimes result in a small convection coefficient (h_c < 2.5 W/m^{2}K), considering a limited temperature difference between wall and air (T<2 °C). This implies a poor heat transfer between the PCM and the indoor environment, and a constrained daily TES in the PCM, which differ from its total storage potential. Liu and Awbi [22] measured the natural convective heat transfer coefficient value of a wall, with and without PCM, obtaining an experimental result of 4.43 and 1.43 W/m^{2}K, respectively. Moreover, special attention should be focused on energy-related occupant behaviour patterns with regard to AC systems. PCM integration should be designed taking into account the specific operation of AC systems, which can be continuous, intermittent or without operation. Every pattern would require different design criteria. Finally, an effective use of PCM requires an appropriate selection of the thermo-physical properties, quantity and position into the building [23].

Different authors have revealed that PCMs incorporated through ventilation systems could overcome reported drawbacks, reducing the amount of PCM and associated cost, increasing heat transfer between PCM and air by forced convection, and insulating PCM during active system operation periods, to take advantage of free cooling at night [9]. Weinläder, Körner and Strieder [24] studied the performance of a ventilated cooling ceiling with PCM, with an airflow rate of 300m^3/h, to improve heat transfer between PCM and air. The ventilated ceiling reduced the maximum operative temperature by up to 2K, compared to the reference scenario. Hu and Heiselberg [25] proposed a ventilated window with a PCM heat exchanger. They concluded that solutions with higher heat transfer rates have a faster thermal response and higher cost saving ability. Santos, Wines, Hopper and Kolokotroni [26] assessed an air handling and heat recovery unit based on a filter, recirculation damper, fan, macro-encapsulated PCM (TES capacity from 6 kWh to 10 kWh) and diffusers. It consists of a technology available on the market called Cool-Phase by Monodraught Ltd [27]. The results reported that internal temperature can be effectively maintained within adaptive thermal comfort limits with reduced costs in comparison to AC systems, and highlighted the importance of PCM selection, airflow rate, heat transfer rate of PCM and TES capacity.

However, despite the reported improvements in passive PCM use, previous research on the assessment of PCM mainly considers short-term evaluation periods and focusses on small-scale testing, not being a more complex integration in buildings commonly addressed. Moreover, some of the reported strategies and design criteria are derived from sensitivity analyses carried out under different boundary conditions. For example, design criteria with regard to PCM layer thickness is dependent on the amount of PCM. Furthermore, there are previous contributions that provide recommendations towards potential benefits without considering the PCM implementation technique and the energy-related occupant behaviour, which highly affect in the final performance and effectiveness of the PCM solution [28]. Thus, the representativeness of associated results and conclusions are limited to specific applications.

As a step forward, this research aims to define criteria and strategies for the effective implementation of latent heat storage solutions towards passive and low-energy cooling in buildings. A novel parametric analysis of two potential PCM implementation techniques is developed, which involves the assessment throughout all cooling demand period under realistic operating conditions. It has been carried out in TRNSYS environment by using the proper boundary conditions and characteristics to support the decision-making process toward an optimal PCM implementation. Solutions are also assessed in two different energy-related operating scenarios (with and without the intermittent operation of air-conditioning systems) with the aim of identifying the required air-conditioning patterns for an optimal PCM use. The two PCM implementation techniques evaluated are: a **conventional passive application (PCM Solution A - direct contact)** based on a PCM layer in contact with indoor space (PCM attached at the ceiling), in which heat transfer between PCM and the air is associated with natural convection; and **an optimised low-energy cooling application (PCM Solution B - indirect contact)** designed as a PCM layer insulated from indoor space (PCM integrated inside the suspended ceiling), in which the air flow is forced by a fan to enhance heat transfer between PCM and the air. A dwelling in a multi-family building in a hot Mediterranean climate was selected as reference scenario for the analyses. This study summaries all design criteria, strategies and requirements for an optimal implementation of PCM towards low-energy cooling solutions and reports key parameters for the development of innovative PCM-based applications.

The paper is structured as follows. First, the reference scenario and the PCM-based solutions are defined, and the selected PCM is characterised. Then, the methodology for numerical simulation is detailed. This was divided into five stages: building modelling, PCM layer, energy systems, operating modes and building performance indicators. Finally, the results are presented and discussed.

2. Reference case study and PCM-based solutions

The performance of conventional and optimised PCM applications is evaluated through three scenarios with two variants. They are summarised in Table 1 and illustrated in Fig. 1. The reference scenario consists of an existing case study without PCM, defined in section 2.1. In this reference case, two applications are studied as alternative PCM solutions: a **conventional passive scenario (PCM Solution A - direct contact)**, based on a PCM layer in contact with indoor space (PCM attached at the ceiling); and an **optimised low-energy cooling scenario (PCM Solution B - indirect contact)**, designed as a PCM layer insulated from indoor space (PCM integrated inside the suspended ceiling). Both solutions were studied without, and with, the simultaneous operation of an active AC system (variant 1 and 2, respectively). In variant 2 (active), AC system is based on an air source heat pump (HP).

Table 1. Summary of scenarios (reference, solution A and solution B) and variants (passive and active)

Scenarios	Variant 1 – No AC system	Variant 2 – With AC system
S0. Reference scenario (basis)	S0v1 - passive	S0v2 - active
S1. PCM solution A – direct contact	S1v1 - passive	S1v2 - active
S2. PCM solution B – indirect contact	S2v1 - passive	S2v2 - active

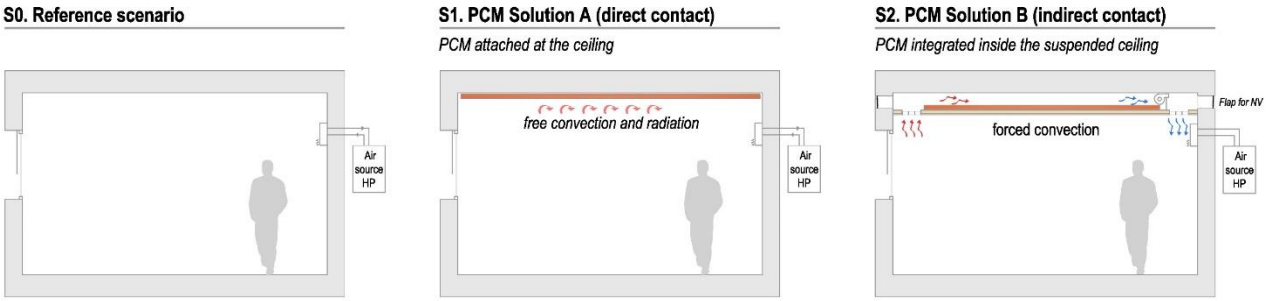

Figure 1. Scenarios assessed: reference scenario - existing case study (S0); PCM solution A - PCM attached at the ceiling (S1); and PCM solution B - PCM integrated inside the suspended ceiling (S2).

In all proposed scenarios, PCM integration is analysed and optimised by sensitivity analysis, with regard to melting temperature, ventilation airflow, amount of material, thickness of PCM layer and different operating patterns.

2.1. Reference scenario

A dwelling in a multi-family building in Seville (Southern Spain), built in 1964, was selected to assess the proposed PCM-based solutions. It is a representative case of the building stock built in the 60s and 70s, before the first national regulation about thermal conditions and energy demand requirements in buildings (NBE-CT-79) [29]. The selected residential unit has 84m^2 (Fig. 2). Seville is characterised by a Mediterranean climate, with relatively mild winters and very warm summers. Monthly mean temperature ranges between 11-13°C in winter, with average minimum and maximum temperatures between 7-9°C and 16-18°C respectively. In summer, monthly mean temperature ranges between 25-29°C, with average minimum and maximum temperatures between 19-22°C and 31-36°C, respectively.

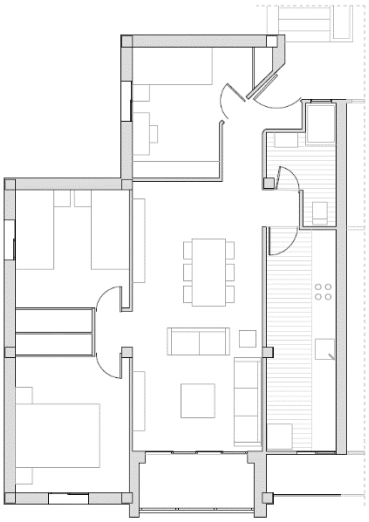

Figure 2. Reference scenario. Dwelling selected for the assessment of proposed PCM-based solutions.

This reference scenario is considered as a single-zone model with changeable occupancy schedules throughout the day, defined in section 3.1. Table 2 shows the main fabric parameters of the case study. This case study is representative of inefficient buildings with a poor thermal envelope. The characterisation of the building energy system is reported in Table 3, based on an air source HP.

Table 2. Characterisation of the fabric elements of the reference case study.

Element	Definition	Characterisation
Window	Simple glazing system with aluminium frames	U-value: 5.7 W/m^2 K
Facade	Solid ceramic bricks, air chamber, simple hollow bricks, cement mortar	U-value: 1.74 W/m^2 K
Internal floor	Terrazzo flooring, structural floor of in-situ joists with ceramic hollow bricks	U-value: 2.60 W/m^2 K
Internal partition	Cement mortar, hollow bricks, cement mortar	U-value: 2.35 W/m^2 K

Table 3. Characterisation of the building energy system of reference case study.

System	Definition	Characterisation
Cooling	Split Air Conditioning based on air-source heat pump	Capacity: 5.3 kW Consumption: 1.54 kW EER: 3.44 Air flow: 32.9 m^3/min (548.3l/s)

2.2. PCM-based scenarios

PCM can be incorporated into the building through different integration techniques. Main applications consist of the integration of macro-encapsulated or microencapsulated PCMs [30]. Microencapsulated PCM, in the form of powder, is usually incorporated into buildings through plaster or cement mortar, concrete or PCM-enhanced drywall, such as gypsum boards [30]. The amount of PCM differs according to the application. Reported concrete solutions may contain about 5% in weight [31]. For gypsum board applications, PCM usually ranges from 26% to 44.5% in weight, according to Oliver, Neila and García [32]. Micronal powder solutions from BASF [33] are the most commonly used. Mean TES capacity of microencapsulated PCM solutions range from 140 to 180 kJ/m^2 for a layer of 15 mm, according to commercial data [34,35]. Macro-encapsulated PCM in panels, spheres, tubes or custom-made products may as well be implemented in buildings. Different solutions are available in the market [36,37]. Mean TES capacity of Macro-encapsulated PCM solutions ranges between 1500 and 3000 kJ/m^2 for a layer of 15 mm.

For this study, macro-encapsulated solutions were selected due to their high TES capacity, following two previously defined different implementation techniques: solution A (direct contact) and solution B (indirect contact).

A reference PCM was selected for the assessment. The thermo-physical properties of the reference PCM are reported in Table 4. It consists of a salt hydrate with high latent heat capacity per unit volume, high thermal conductivity (double that of paraffin), and little volume change during melting [19]. The selected inorganic component, SP26E from Rubitherm, is characterised by a melting temperature of 26 ºC and a heat storage capacity of approximately 180kJ/kg. Partial enthalpy distribution and total enthalpy evolution, through the course of the melting and crystallisation processes, are illustrated in Fig. 3, showing the need of sub-cooling for crystallisation of approximately 1ºC.

Table 4. Thermo-physical properties of selected PCM (SP26E).

Properties	Characterisation
Melting temperature (ºC)	26 (25-27)
TES capacity (kJ/kg)	180
Thermal conductivity (W/m K)	0.6
Specific heat (kJ/kg K)	2
Density in solid phase (kg/m^3)	1500
Density in liquid phase (kg/m^3)	1400

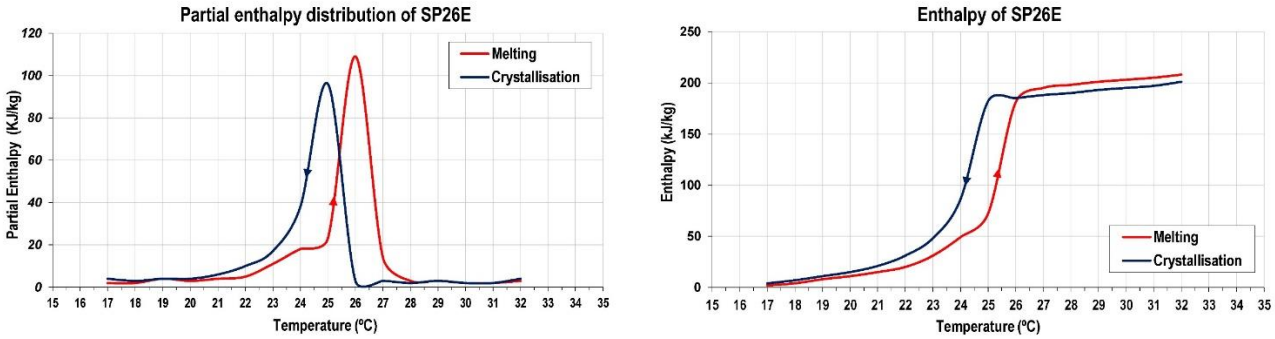

Figure 3. Partial enthalpy distribution and total enthalpy throughout the melting and crystallisation processes of selected PCM (SP26E).

3. Methodology for numerical simulation

The numerical simulation was carried out in the energy system simulations software TRNSYS (Transient System Simulation) v18 [38]. TRNSYS is a flowsheet simulator with a graphical interface which facilitates the decomposition of complex problems into various, interconnected model components. TRNSYS implements algebraic and first-order ordinary differential equations, describing physical components into software subroutines, with a standard interface. The TRNSYS model library includes components for the calculation of building thermal loads, ventilation and air-conditioning (HVAC) systems, as well as climatic data files, making it a very suitable tool to model air-conditioning installations for heating and/or cooling. The validation of the numerical model was carried out according to the criteria defined in ASHRAE Guideline 14-2014 [39]. The uncertainty indices used for model validation are the Normalized Mean Bias Error (NMBE), the Coefficient of Variation of the Root Mean Square Error (CV-RMSE) and the Coefficient of determination (R^2). NMBE is a normalization of the MBE index that is used to scale the results, making them comparable; CV-RMSE measures the variability of the errors between measured and simulated values; and R^2 indicates how close simulated values are to the regression line of the measured values [40]. ASHRAE Guideline recommends that for a good reliability, the simulation model shall have an NMBE lower than 5% and CV-RMSE lower than 15% relative to monthly calibration data. If hourly calibration data are used, these requirements shall be 10% and 30%, respectively. Additionally, it is recommended to obtain a value of R^2 higher than 0.75. The reference building scenario (case study without PCM) was validated with data obtained from monthly energy bills, and the PCM model component was validated using experimental data. Moreover, a sensitivity analysis to assess the effect of most relevant parameters in numerical model performance was developed in order to ensure the reliability of the conclusions derived from this study.

The simulation modelling is divided into five sections, illustrated in Fig. 4: building modelling, PCM layer, energy systems, controller of operating modes and building performance indicators. In the next subsections, the numerical procedures used in each section are further described.

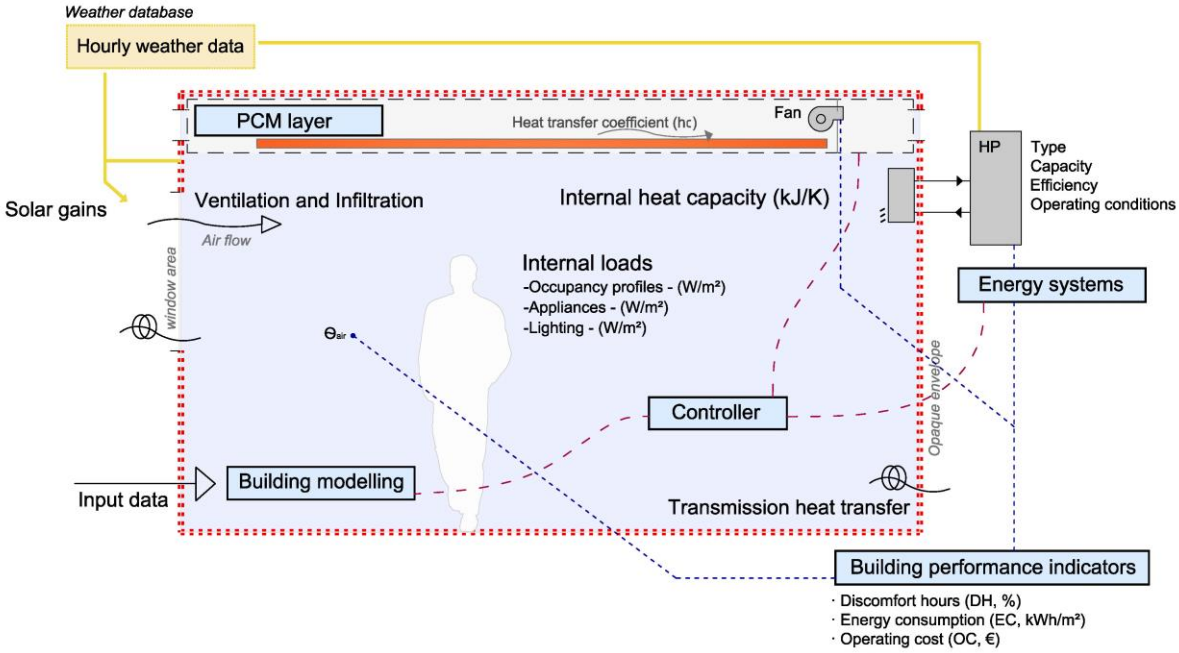

Figure 4. Scheme of the methodology for numerical simulation. Relationship between the numerical model sections: building modelling, PCM layer, energy systems, controller and building performance indicators.

3.1. Building modelling

The case study, previously defined in section 2.1, was modelled as a single-zone and implemented as a component in TRNSYS Simulation Studio (TYPE 56). The geometric definition of the model reproduces the existing form, window surfaces and external shadings. The dwelling was further characterised through TRNSYS TRNBuild, including building elements (walls, floors, ceilings, roofs and windows), occupancy schedules, infiltration, ventilation rates and internal gains, among other aspects. Weather profiles for Seville (Spain) were generated using Meteonorm from the data base of Meteotest and implemented within TRNSYS using the standard weather data reader component (TYPE 15-2).

Occupancy schedules and heat flow rates of internal gains are shown in Fig. 5. Two different occupancy schedules were implemented: a weekday profile and a weekend profile. Total heat flow rate from occupants ($\Phi_{int,oc}$) depends on their metabolic activity (met) and the occupancy density (m²/person) of the conditioned area. The metabolic rate of occupants during common residential activities ranges from 0.8 to 1.2 met (from 46 to 70 W/person), according to ISO 7730:2005 [41]. Thus, the specific heat flow rate from occupants was characterised at 3.52 W/m², being weighted per hour, according to occupancy schedules, taking regional standards as reference [42]. Specific heat flow rates from appliances ($\Phi_{int,ap}$) and lighting ($\Phi_{int,li}$) are considered using an additional schedule, ranging from 0.44 to 4.4 W/m² according to Annexe G of ISO 13790:2008 [43], and other technical manuals and references [42,44].

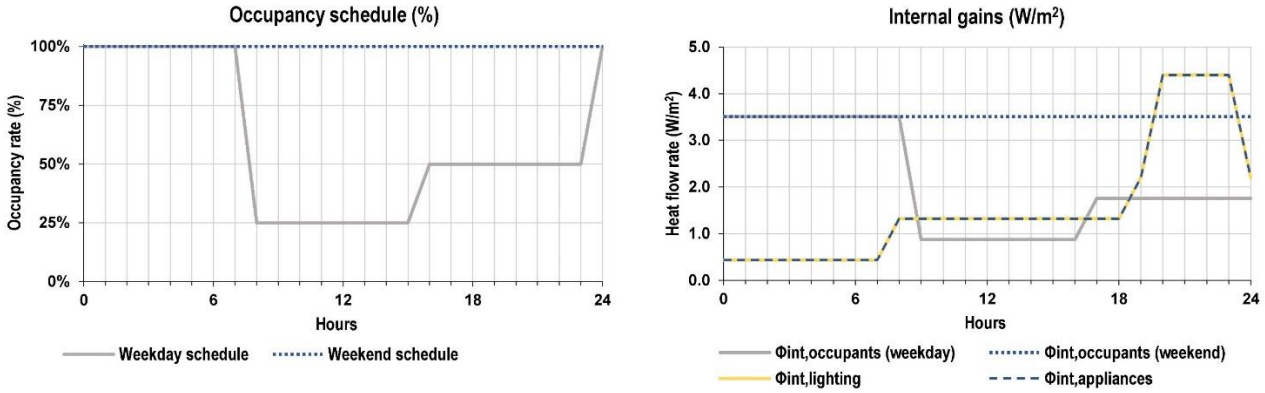

Figure 5. Occupancy schedules and internal gains of numerical simulation model.

Infiltration leakage is defined by an air change rate (ACH) of 1.2 h^{-1} at 4Pa, corresponding to an ACH at 50 Pa (n50) of 6.5 h^{-1}, according to the procedure defined in Annex A.2 of EN 13465 [45]. This value lies within the range of typical levels of ACH of between 5.6 h^{-1} and 9.4 h^{-1} (n50), reported by Escandón, Suárez and Sendra [46], due to infiltrations in multi-family buildings built between the 1960s and 1980s in southern Europe. The assumed infiltration leakage is also similar to recommended values for multi-family buildings, with medium-high leakage levels, reported in Annexe B of EN 15242:2007 [47].

Natural ventilation, from window openings throughout summer nights, was calculated according to Eq. 1 and 2, defined in EN 15242 [47], considering window opening surface area, wind speed and air temperature differences.

$$Q_v = 3.6 \cdot 500\, A_{ow} V^{0.5} \quad (1)$$

$$V = C_t + C_w \cdot V_{met}{}^2 + C_{st} \cdot H_{window} \cdot abs\,(\theta_i - \theta_e) \quad (2)$$

where:

Q_v: air flow (m³/h)
A_{ow}: window opening area (m²)
C_t: takes into account wind turbulence (0.01)
C_w: takes into account wind speed (0.001)

V_{met}: meteorological wind speed at 10 m height
C_{st}: takes into account stack effect (0.0035)
H_{window}: free area height of the window
Θ_i: room air temperature
Θ_e: outdoor air temperature

Thermal bridges are characterised at 0.1 W/m²K of envelope area [43]. The internal heat capacity of the building model is fixed to 1530kJ/K. This value results from an indoor air volume thermal capacitance of 255kJ/K, and an effective heat capacity for furniture and internal walls of 1275kJ/K (17kJ/Km²), taking the average data reported by the following publications and manuals as reference. Johra and Heiselberg [48], who studied the influence of internal thermal mass in building simulations, reported that total internal heat capacity is usually considered by multiplying the indoor air volume thermal capacitance of the model by a constant value, ranging from 3 to 8, according to the building use. The TRNSYS software guideline advises a value ranging between 3 and 5 in some examples [49]. Johra and Heiselberg [48] collected effective heat capacities from different authors for low, medium and heavy furnishing, showing values from 17 to 45 kJ/Km² of floor area.

The building model validation is carried out according to monthly energy bill data throughout the summer period. The results of uncertainty indices are reported in Table 5.

Table 5. Comparison between the measured and simulated values and uncertainty indices for building model validation according to ASHRAE Guideline 14-2014.

Month	Measured (kWh)	Simulated (kWh)	Difference (kWh)	ASHRAE 14 criteria
June	125	101	24.10	
July	313	291	21.43	
August	292	310	-18.03	
September	100	152	-52.17	
		NMBE	-2.97 %	±5%
		CV-RMSE	6.87 %	< 15%
		R^2	0.89	> 0.75

The results show a deviation between the monthly values obtained with measurements and numerical simulation below 5% in NMBE and less than 15% in CV-RMSE. Additionally, a value of R^2 higher than 0.75 is obtained. So, the numerical model meets the criteria of ASHRAE guideline 14-2014 [39], achieving the calibration results of NMBE -2.97%, CVRMSE 6.87% and R^2 0.89.

3.2. PCM layer

Different procedures and TYPES can be found in literature for PCM modelling in TRNSYS [50–52]. For these specific applications, the PCM layer was characterised using TYPE 399 [53]. This component was developed by Dentel and Stephan [54], and it allows the simulation of different PCM-enhanced building components, such as PCM wall, ceiling or panels [55]. The TYPE can also model passive and active PCM applications due to the algorithm includes a resistance network for capillary tube.

The mathematical model structure is based on the Crank-Nicolson method, solving the heat conduction equation by elimination method, as described in [54]. The discretisation scheme is one-dimensional. PCM characteristics can be modelled through a temperature-dependent heat capacity, considering the hysteresis effect of the PCM by using two separate enthalpy curves for melting and freezing. Thus, the enthalpy changes are implemented as an invertible function of the temperature, using two data files. Used PCM data was previously defined in Section 2.2 for melting and freezing. Finally, the TYPE 399 is coupled with the TYPE 56 (building model) of TRNSYS by defining and connecting the boundary conditions of the simulated room with the PCM component.

As mentioned above, the convective heat transfer coefficient (h_c) between PCM-air has an important role in final solution performance. For the specific case of natural convection in Solution A – direct contact, h_c is automatically calculated by TRNSYS, resulting in values ranging from 3 to 4 W/m² K. In the Solution B – indirect contact, h_c is enhanced by the airflow forced by a fan. It depends mainly on the air flow properties (velocity and regime) and PCM surface characteristics (geometry and rugosity), as well as their thermal properties. In this study, the specific h_c value due to forced airflow over a PCM flat surface is calculated according to Eq. 3 reported by [56] as a function of wind velocity.

$$h_{fc} = a + bV = 2.8 + 3V \text{ (for } 0< V <7\text{m/s)} \quad (3)$$

Where
$h_{c,f}$*: forced convective heat transfer coefficient (W/m²K)*
V*: wind velocity (m/s)*

For an air velocity of 4m/s, h_c between PCM-air results in 15W/m², a conservative value considering the results reported from previous studies. Yanbing, Yi and Yinping [57] measured the h_c between PCM and air with forced ventilation, obtaining values of between 12 and 19 W/m² K. Hed and Bellander [58] showed that h_c between the air and PCM increases significantly when the surface is rough, compared to a smooth surface, ranging from 16 to 30 W/m² K for an air velocity of 4m/s.

The PCM model is validated using the experimental data reported by Castell et al. [59], in which similar PCM layers for passive cooling were experimentally tested in cubicles. The energy model was characterised according to the boundary conditions of cubicles for both tested scenarios (with and without PCM); and the PCM layer was defined according to the specific material used (SP-25 A8). The results of measured and simulated values are illustrated in Fig. 6, and associated uncertainty indices, according to ASHRAE guideline, are summarized in Table 6.

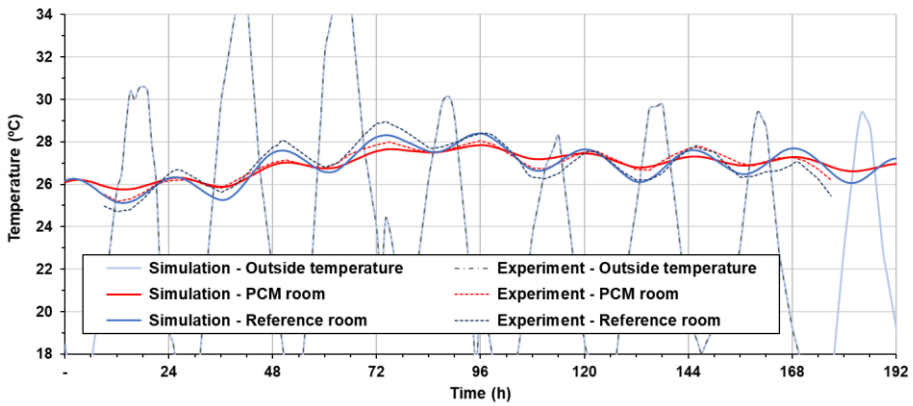

Figure 6. Comparison between the experimental and simulated results.

Table 6. Uncertainty indices used for PCM model validation according to ASHRAE Guideline 14-2014.

Uncertainty indices	PCM room	Reference room	ASHRAE 14 criteria
NMBE	0.08 %	0.02 %	±10%
CV-RMSE	1.06 %	0.23 %	< 30%
R^2	0.91	0.85	> 0.75

Following the ASHRAE guideline 14-2014 procedure [39], the energy model achieves the calibration results of NMBE 0.08%, CVRMSE 1.06% and R^2 0.91 in the PCM cubicle scenario; and NMBE 0.02%, CVRMSE 0.23% and R^2 0.85 in the reference cubicle scenario, meeting the ASHRAE criteria and ensuring the reliability of the PCM numerical model.

3.3. Energy systems

Active AC systems implemented within the simulations were modelled using different components (or Types) in TRNSYS Simulation Studio. The single-zone is linked to an air source heat pump (HP), modelled using TYPE 954. The performance of HP is characterised by its cooling capacity (kW) and energy efficiency ratio (EER). These data refer to rated (nominal) operation conditions (Eurovent certification values). Correction functions are used to adapt rated operation data at nominal conditions to real operating conditions. Other components used for specific scenarios were fans (TYPE 662), mixing valves (TYPE 648), and different standard controllers and utilities. The simulation time step was set at 90 seconds.

3.4. Controlling of operating modes

3.4.1. Conventional controller for the reference scenario

A conventional controller manages the operating mode of HP for cooling within the base scenario, in variant 2, with combined participation of an active system. The system operation follows an intermittent schedule linked to the defined occupancy pattern. The HP is automatically activated if the occupancy rate is ≥50%, following a cooling set-point temperature of 25° C and 27° C for daytime and night, respectively.

3.4.2. Controller for PCM-based scenarios

A more complex controller was implemented within the PCM-based scenarios. It manages the HP for active cooling in both PCM-based solutions and the air chamber ventilation in Solution B (indirect contact). As a result, three different operating modes for passive and active conditioning were implemented, which are illustrated in Fig. 7.

- Operating mode 1 - Charging PCM (passive): PCM absorbs heat gains during the day, melting. Solution A is characterised by natural convection, and solution B by forced convection induced by a fan, which forces the warm indoor air from the room into the air chamber of the suspended ceiling where the PCM is located.

- Operating mode 2 - Discharging PCM (passive): PCM releases stored heat due to night free cooling, solidifying. Solution A is characterised by natural ventilation through window openings, and in solution B a fan forces the cool outside airflow into the suspended ceiling where the PCM is located.

- Operating mode 3 - HP cooling (active): HP is automatically activated if the occupancy rate is ≥50%. In solution B, through the course of this operating mode, the flaps of the suspended ceiling are closed, insulating the PCM from the indoor environment.

Two PCM-based solutions were assessed for two variants: **variant 1 (passive)** with only passive operating modes (mode 1 and 2), and **variant 2 (active)**, with passive and active operating modes (mode 1, 2 and 3).

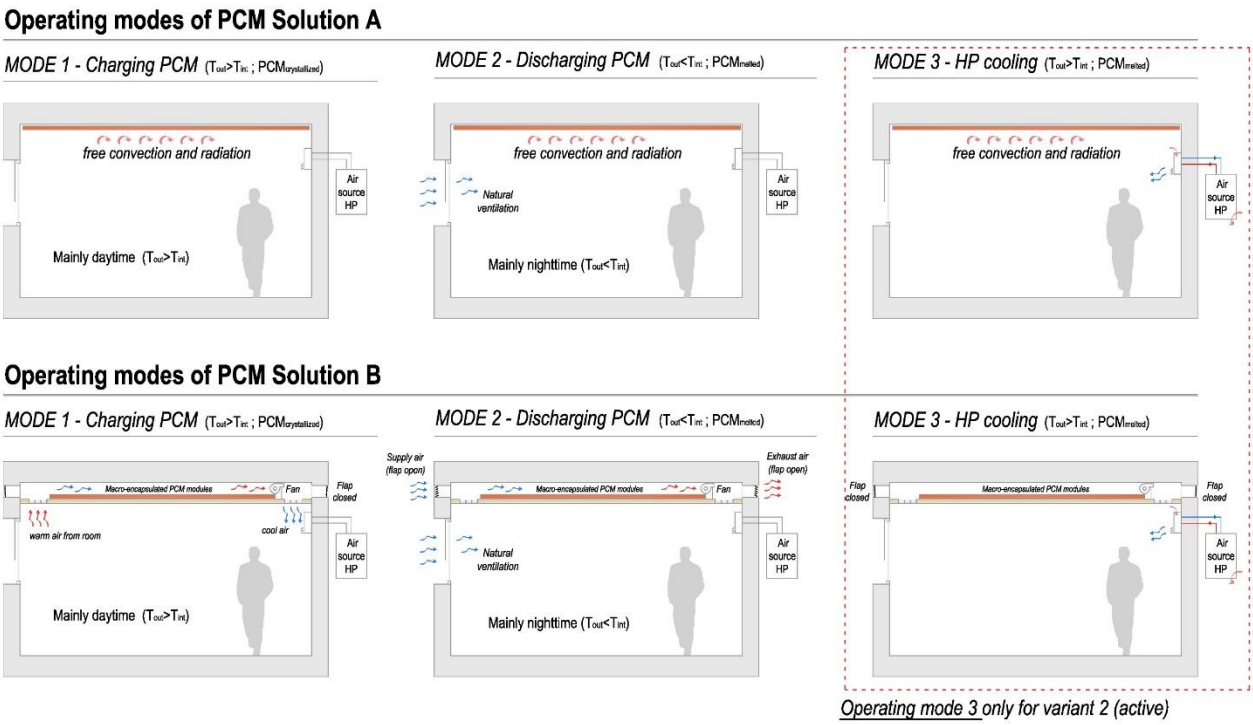

Figure 7. Operating modes of proposed PCM-based solutions: mode 1 - charging PCM; mode 2 - discharging PCM; and mode 3 - direct HP cooling (only for variant 2 – active)

3.5. Building performance indicators

Building energy performance of the proposed PCM-based solutions compared to the reference scenario was evaluated through different key performance indicators.

PCM-based solutions in variant 1 (passive), where alternatives are simulated with free temperature oscillation (no active AC system), were evaluated through the percentage of discomfort period, during the summer season (from June 21 to September 23), based on the following procedures:

- **Percentage of severe discomfort hours** (DH, %) with indoor operative temperature above 29ºC.

- **Percentage of discomfort hours** (DH_{acm}, %) considering the comfort range of the adaptive thermal comfort model established in the new draft revision of EN 15251 [60], which has been renamed with the code prEN 16798-1 [61]. It is a thermal comfort analysis that considers user expectation and their interaction with the building. Acceptable operative temperature levels are based on outdoor temperature. Selected range of operative temperatures corresponds to comfort category I, which is associated to a high level of expectation (PPD < 6%), and is determined by a temperature interval of +2K *(upper limit)* and -3K *(lower limit)*, in relation to the indoor comfort operative temperature (T_{co}), calculated by applying Eq. 4.

$$T_{co} = 0.33 \cdot \Theta_{rm} + 18.8 \quad (4)$$

where Θ_{rm} is the running mean external temperature, calculated by using Eq. 5.

$$\Theta_{\mathrm{rm(ed)}} = (\Theta_{ed-1} + 0.8 \cdot \Theta_{ed-2} + 0.6 \cdot \Theta_{ed-3} + 0.5 \cdot \Theta_{ed-4} + 0.4 \cdot \Theta_{ed-5} + 0.3 \cdot \Theta_{ed-6} + 0.2 \cdot \Theta_{ed-7})/3.8 \quad (5)$$

where:
$\Theta_{rm(ed)}$: mean external temperature of focus day.
Θ_{ed-1}: daily mean outdoor air temperature for n-days prior to focus day.

PCM-based solutions in variant 2 (active), where alternatives are simulated with an intermittent operation of AC systems, were evaluated through the cooling energy consumption and its associated operating cost, during summer season (from June 21 to September 23):

- **Cooling energy consumption** (EC, kWh/m^2) was evaluated through the specific final energy consumption of the building, associated with the AC system and the fan, for enhancing ventilation in the suspended ceiling. It is related to the conditioned floor area (Af) in order to facilitate the comparison of the energy performance with other buildings.

- **Operating cost** (OC, €) was evaluated according to the hourly energy consumption of the AC and ventilation systems, that operate using a standard electricity tariff.

4. Simulation results and discussions

The optimisation of PCM-based solutions is analysed and discussed in three steps. Firstly, the energy performance of the reference scenario is described, identifying different design and sizing alternatives for PCM implementation. Secondly, the results of a parametric analysis carried out for optimising the PCM design are presented. This sensitivity analysis involves the study of melting temperature (ºC), area of window opening (m^2), or fan airflow rate (m^3/h) for NV, the amount of PCM (TES capacity in kWh) and thickness of PCM layer. Finally, the results of optimised PCM-based solutions are shown and compared.

4.1. Reference scenario and design and sizing alternatives for PCM-based solutions

The results of **Reference scenario - variant 1 (passive)** show a discomfort period based on T_{op}>29ºC (DH) and an adaptive comfort model (DH_{acm}), of 38% and 27%, respectively. The results of **Reference scenario - variant 2 (active)** show a cooling energy consumption of 11.4 kWh/m^2 and an associated operating cost of 100€.

Figure 8 illustrates the evolution of maximum and minimum daily temperature of **Reference scenario for variant 1 (passive) and variant 2 (active)**, throughout the summer period. It allows supporting the selection of PCM melting temperature according to climate requirements.

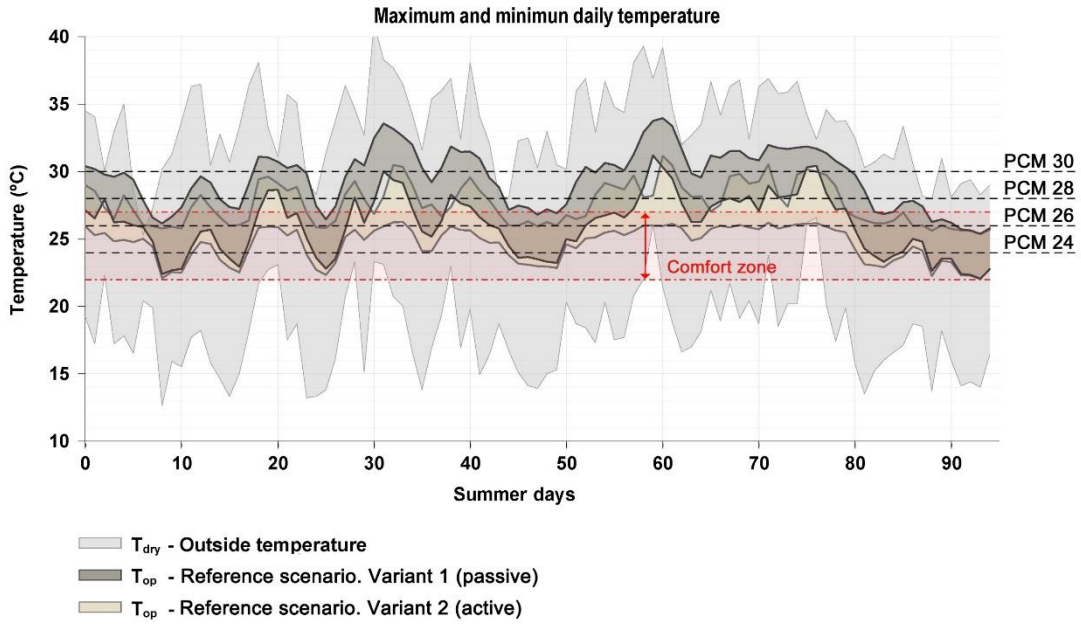

Figure 8. Maximum and minimum daily temperature of reference scenario in variant 1 (passive) and variant 2 (active) throughout the summer season, compared with outside temperature oscillation (T_{dry}) and the different alternatives of PCM melting temperature (PCM 30, 28, 26 and 24).

For this reference case study, four PCM melting temperature alternatives can be considered (Table 7): 30ºC, 28ºC, 26ºC and 24ºC. They encompass indoor temperature oscillation achieved throughout most summer days. Thermo-physical properties of the PCM alternatives are considered identical to SP26E. Just partial enthalpy distribution was modified to achieve selected melting temperatures.

Table 7. Design alternatives of PCM melting temperature.

Nomenclature	Melting temperature (ºC)	TES capacity (kJ/kg)
PCM 24	24	180
PCM 26	26	180
PCM 28	28	180
PCM 30	30	180

Fig. 9 illustrates the load duration curve (LDC), which shows the relationship between cooling capacity requirements (kW) and capacity utilisation hours. The existing cooling system has a capacity of 5.3 kW, being able to cover 98% of required cooling capacity.

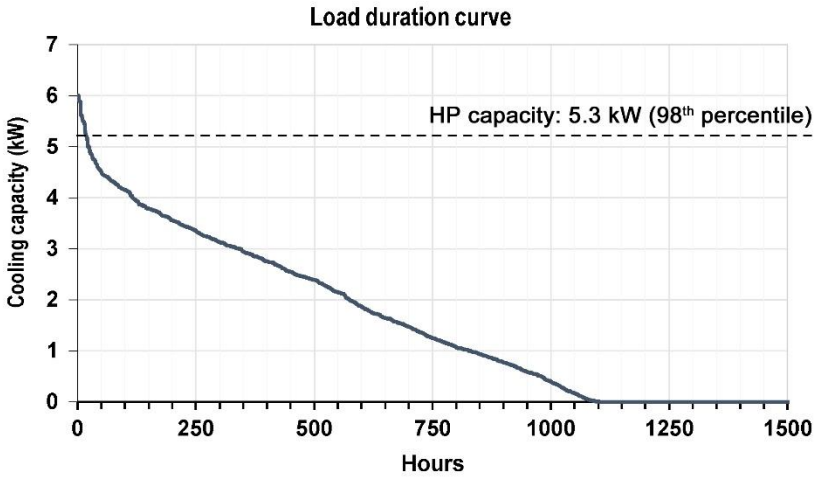

Figure 9. Load duration curve per number of hours in the reference case study. Sizing of HP capacity.

In **PCM Solution A (direct contact)**, due to the importance of NV for PCM regeneration at night during summer period, different window opening behaviours are studied (Table 8). The reference case study is evaluated with a window opening area of 2m^2 for all summer nights, which results in air changes ranging from 3 to 6.5 h^{-1} according to the hourly wind speed, with a mean value of 3.4 h^{-1}.

Table 8. Alternatives of window opening area for NV in scenario S1 (PCM Solution A)

Nomenclature	Window openings (m^2)	Mean NV (h^{-1})
A_{ow} 1	1	1.8
A_{ow} 1.5	1.5	2.6
A_{ow} 2	2	3.4
A_{ow} 2.5	2.5	4.2

In **PCM Solution B (indirect contact)**, four sizing alternatives for fan airflow can be considered (Table 9). It should be taken into account that higher airflow represents an increase in electricity consumption.

Table 9. Sizing alternatives of airflow rate and associated energy consumption in scenario S2 (PCM Solution B).

Nomenclature	Air flow of fan (m^3/h)	Power (kW)
Airflow 415	415 (486 kg/h)	0.062 kW
Airflow 880	880 (1030 kg/h)	0.084 kW
Airflow 1275	1275 (1492 kg/h)	0.104 kW
Airflow 1575	1575 (1843 kg/h)	0.119 kW

Fig. 10 illustrates the relationship between daily cooling demand (kWh) per number of days in the reference case study, which allows defining the amount of PCM required to absorb most daily heat gains. For this reference case study, four alternatives of TES capacity, of 75, 55 and 35 and 15 kWh, can be considered (Table 10), which cover 98%, 95%, 80% and 40% of days, respectively, considering that the PCM could be completely regenerated at the beginning of each day.

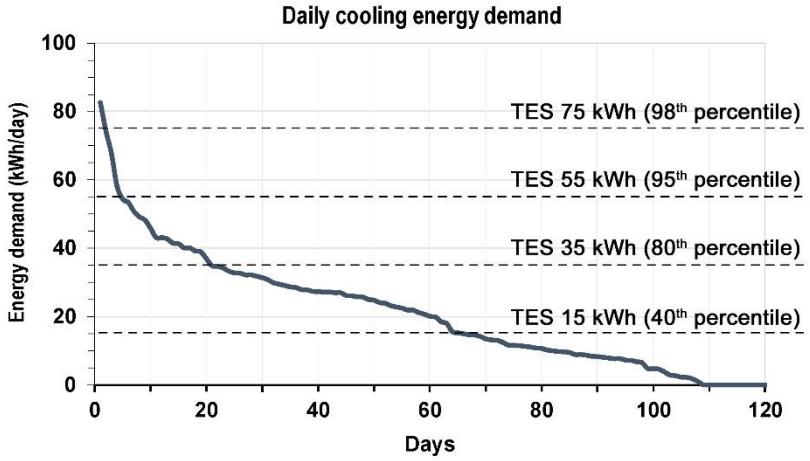

Figure 10. Daily cooling energy demand of the reference case study.

Table 10. Sizing alternatives of amount of PCM (m^3) according to TES capacity (kWh).

Nomenclature	TES capacity (kWh)	Amount of PCM (m^3)	Layer thickness (mm)	Layer surface (m)
TES 15	15	0.25	10	25
TES 35	35	0.5	10	50
TES 55	55	0.75	10	75
TES 75	75	1	13.5	75

4.2. Parametric analysis for system optimisation

Fig. 11 illustrates the parametric analysis of the two proposed **PCM-based solutions (A and B) in the variant 1 (passive),** considering different design and sizing alternatives for PCM implementation, previously mentioned in section 4.1, according to PCM melting temperatures (ºC), areas of window opening (m^2), or fan airflow rates (m^3/h) for NV, the amount of PCM (TES capacity in kWh), and thickness of PCM layer (mm). The red line identifies the alternative selected in each step in the sensitivity analysis.

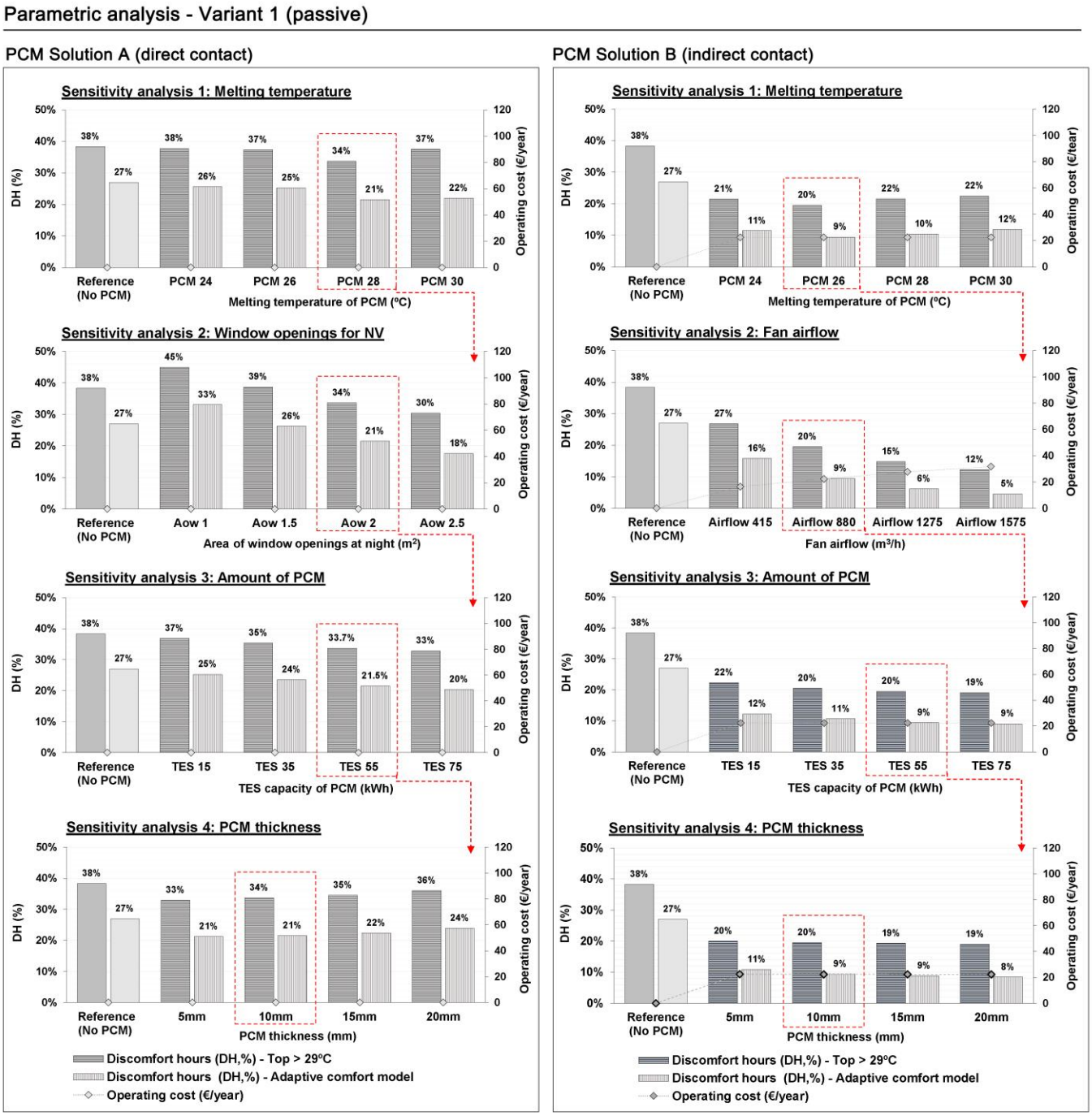

Figure 11. Parametric analysis of both PCM solutions (A and B) in the case of variant 1 (passive, without air-conditioning systems). Sensitivity analysis with regard to PCM melting temperatures (1), areas of window opening or fan airflow rates for NV (2), the amount of PCM (3), and thickness of PCM layer (4).

- **PCM melting temperature** is one of the most relevant parameters for the success of the application. The sensitivity analysis in the variant 1 (passive) shows that for **PCM Solution A (direct contact)**, the most appropriate melting temperature is 28ºC, and for **PCM Solution B (indirect contact)**, it is 26ºC. As mentioned in other studies, making general assumptions is not recommended [15,16]. An inappropriate phase change temperature could mean that PCM is melted or solidified, most of the time, without providing any latent heat storage process. PCM melting temperature selection depends on internal gains, climate conditions, and lower indoor temperatures, that can be achieved by night ventilation [14].

- **Night ventilation** is emphasised as essential for the effective regeneration of TES material at the beginning of each day, as reported by different authors [16]. **Both PCM-based solutions in variant 1 (passive)** show that the higher the ventilation rates achieved at night (through natural ventilation or fan airflow), the lower the obtained discomfort periods are. This is because PCM can release most of the absorbed heat of the previous day, increasing the TES capacity to modulate temperature rise. However, it should be considered that the window opening area of **PCM solution A (direct contact)** is manually controlled by the occupants; and increasing fan airflow of **PCM solution B (indirect contact)** will more frequently keep internal temperatures within the comfort range, but with a higher electricity consumption penalty, which could make it less attractive. An attractive improvement for **PCM solution A** could be the implementation of indoor and outdoor temperature sensors for the automatic operation of windows, which could efficiently increase natural ventilation rates, when required. In addition, increasing airflow rate in **PCM solution B** could lead to increased heat transfer rate between PCM and air, due to the better airflow characteristics. Thus, associated configurations don't only affect the final night ventilation rate, but also the heat transfer capacity between PCM and air.

- **TES capacity** of solutions is another key parameter which can limit the benefits of free cooling strategies. It should be appropriately designed according to daily cooling needs. If a higher than required TES capacity is defined, it will not provide greater benefits, and it will suppose larger space requirements and costs. Optimal configurations are found between 35 and 55 kWh for both solutions, which represent a 95^{th} and 80^{th} percentile of daily cooling needs.

- **The thickness of PCM layer** (considering the same amount of PCM) is another design parameter with influence in final performance of solutions because of the different contact area between PCM and air. In PCM solution A, higher layer thickness reduces the PCM surface, decreasing heat transfer capacity of solution, and providing worse performance. On the other hand, the parametric analysis reveals that increasing thickness in PCM solution B, the discomfort hours are reduced, being directly associated to lower heat transfer capacity along the storage period (without fan operation). So, PCM reduces heat losses until the fan operation, which increases heat transfer rate through forced convection.

Fig. 12 illustrates the parametric analysis of the two proposed **PCM-based solutions (A and B) in variant 2 (active),** considering different design and sizing alternatives for PCM implementation, previously mentioned in section 4.1, according to PCM melting temperatures (ºC), areas of window opening (m^2), or fan airflow rates (m^3/h) for NV, the amount of PCM (TES capacity in kWh) and thickness of PCM layer (mm). The red line identifies the alternative selected in each step in the sensitivity analysis.

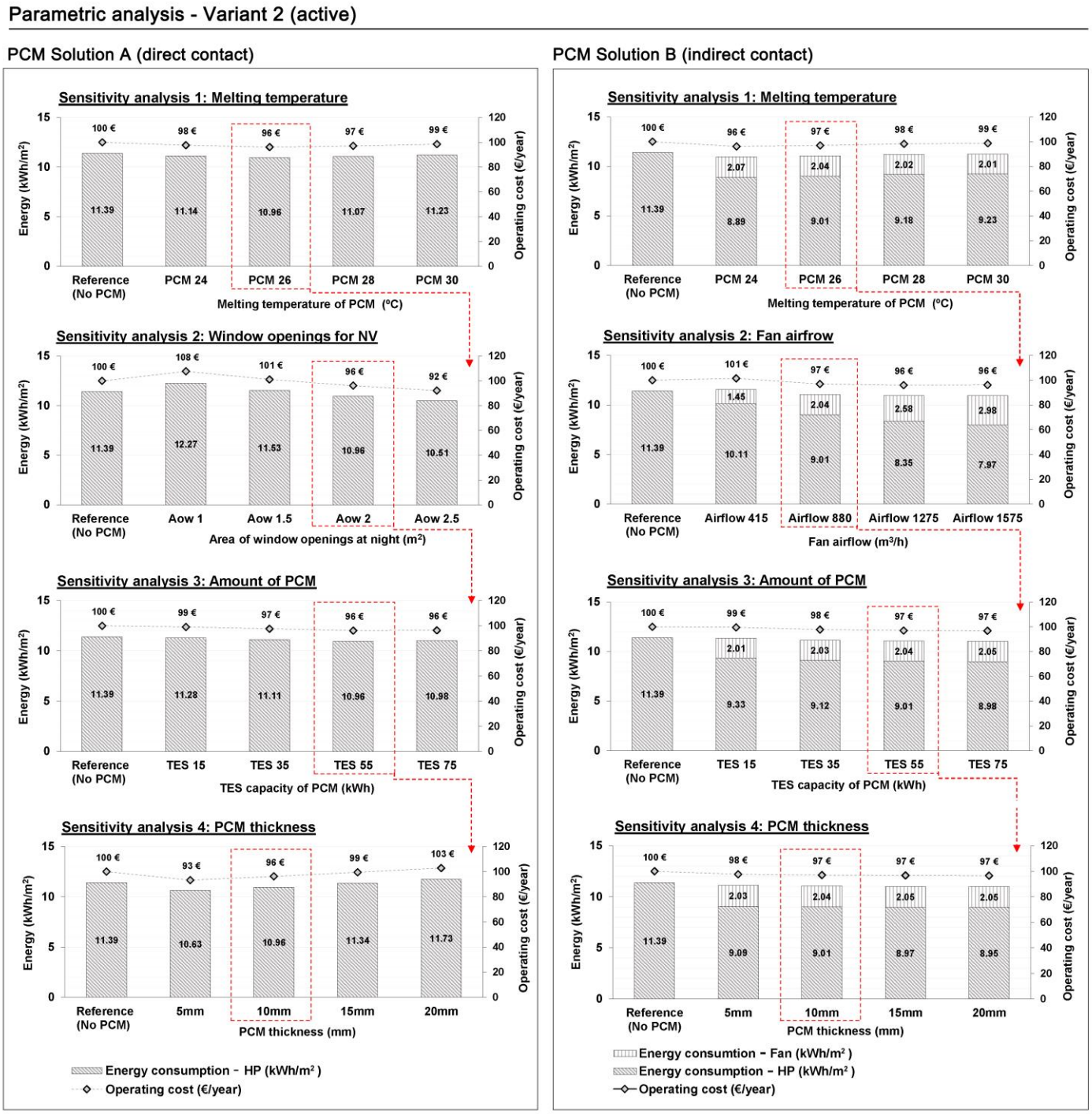

Figure 12. Parametric analysis of both PCM solutions (A and B) in the case of variant 2 (active, with air-conditioning systems). Sensitivity analysis with regard to PCM melting temperatures (1), areas of window opening or fan airflow rates for NV (2), the amount of PCM (3), and thickness of PCM layer (4).

The results of **PCM-based solutions (A and B) in the variant 2 (active)** show that the benefits provided by the PCM with the intermittent operation of AC systems are limited because of the following issues:

- **In PCM Solution A (direct contact)**, the heat absorbed during the day by the PCM cannot be released at night, due to the intermittent operation of AC system in the afternoon. As a consequence, the results on final energy consumption and associated operating costs are close to those of the **Reference scenario**, with no benefits by the implementation of the proposed PCM-based alternatives.

- **In PCM Solution B (indirect contact)**, the heat absorbed during the day by the PCM can be efficiently released during the night. The simulation results show a reduction of energy consumption associated with the heat pump of 21%. It is also shown that an increment of the fan airflow rate would enable additional savings, related to the HP consumption. Nonetheless, due to the fan's energy consumption, final energy consumption and associated operating results would be almost similar to the values obtained in the **Reference scenario**.

4.3. Results of optimised PCM-based cooling solutions

Once the PCM integration has been optimised by sensitivity analysis in two proposed PCM-based scenarios, final performance is summarised as follows.

Figures 13 and 14 illustrate the final performance of the proposed **PCM-based solutions (A and B) in the variant 1 (passive)**, with free temperature oscillation (no AC system operation). Fig. 13 shows the percentage of discomfort hours based on indoor operative temperature above 29ºC (DH, %) and adaptive comfort model (DH_{acm}, %), and Fig. 14 represents the evolution of maximum and minimum daily temperature, throughout summer period.

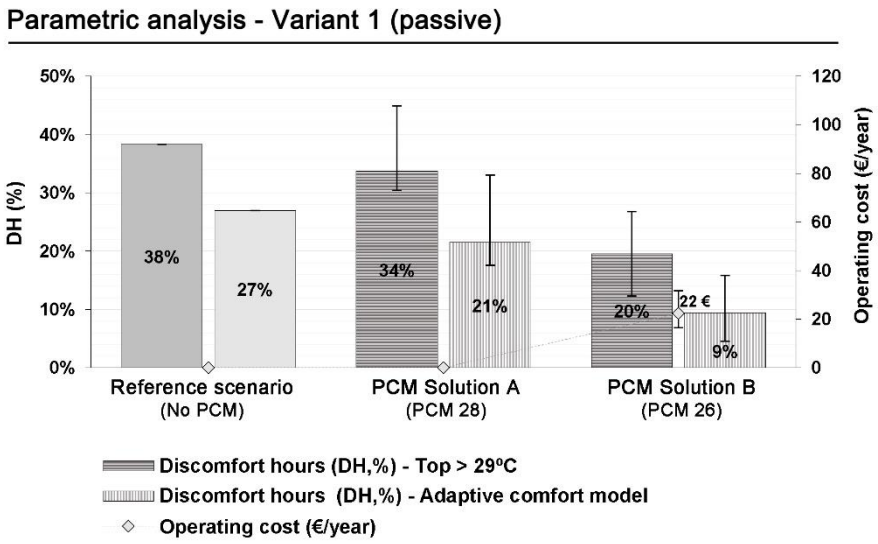

Figure 13. Results of optimised PCM-based solutions (A and B) in the case of variant 1 (passive, without air-conditioning systems), compared with the reference scenario (no PCM).

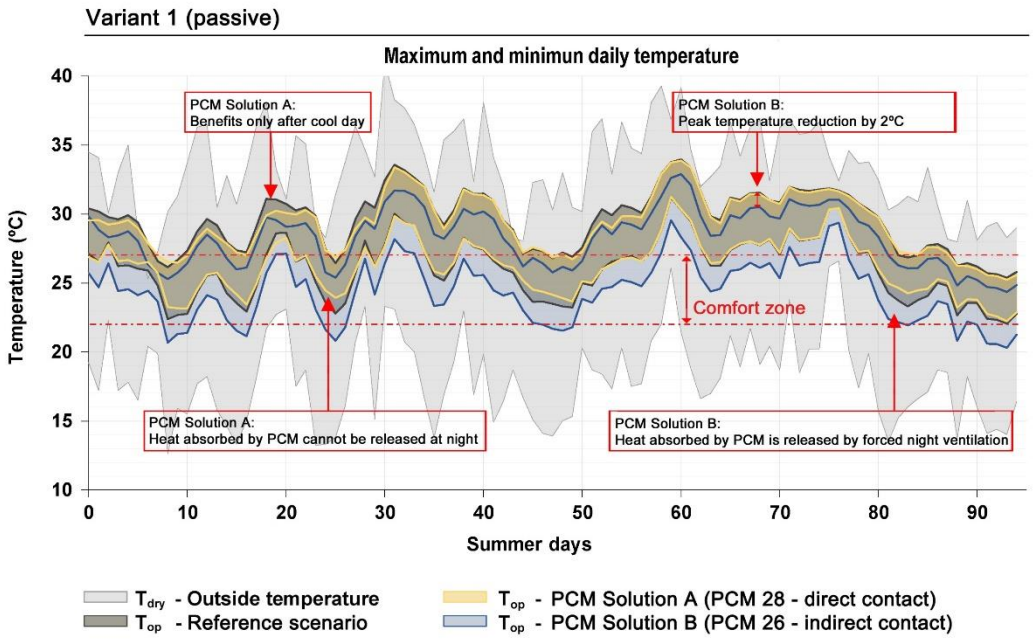

Figure 14. Maximum and minimum daily temperature of optimised PCM-based solutions (A and B) in the case of variant 1 (passive, without air-conditioning systems), compared with outside temperature oscillation (T_{dry}) and the reference scenario without PCM (T_{op}).

- **PCM Solution A (direct contact) in variant 1 (passive)** results in a reduction in discomfort period based on T_{op}>29ºC, and an adaptive comfort model of 12% (from 38% to 34%) and 20% (from 27% to 21%), respectively. Its limited benefit is related to the low heat transfer between PCM and air, mainly associated with natural convection, which limits the heat storage in the material. It means that heat absorbed by the PCM cannot be released at night during most days, and the reduction of discomfort hours is only performed in periods after very cool days (see Fig. 14).

- **PCM Solution B (indirect contact) in variant 1 (passive)** results in a reduction of severe discomfort hours (T_{op}>29ºC) of 49% (from 38% to 20%), and the discomfort period defined by adaptive comfort model of 65% (from 27% to 9%). Heat absorbed by the PCM during daytime can be efficiently released by forced night ventilation, and peak operative temperature is reduced by up to 2 K, compared to the reference case study of most days of summer (see Fig. 14). In addition, it is highlighted that with improved heat transfer techniques, based on better flow properties (velocity and regime), and surface characteristics (geometry and rugosity), produce a reduction in the discomfort period based on T_{op}>29ºC, and that an adaptive comfort model of up to 68% and 83% can be achieved, respectively.

Figures 15 and 16 illustrate the final performance of the proposed **PCM-based solutions (A and B) in the variant 2 (active)**, with the intermittent operation of AC systems. Fig. 15 shows the energy consumption and associated operating cost of AC system, and Fig. 16 represents the evolution of maximum and minimum daily temperature, throughout summer period.

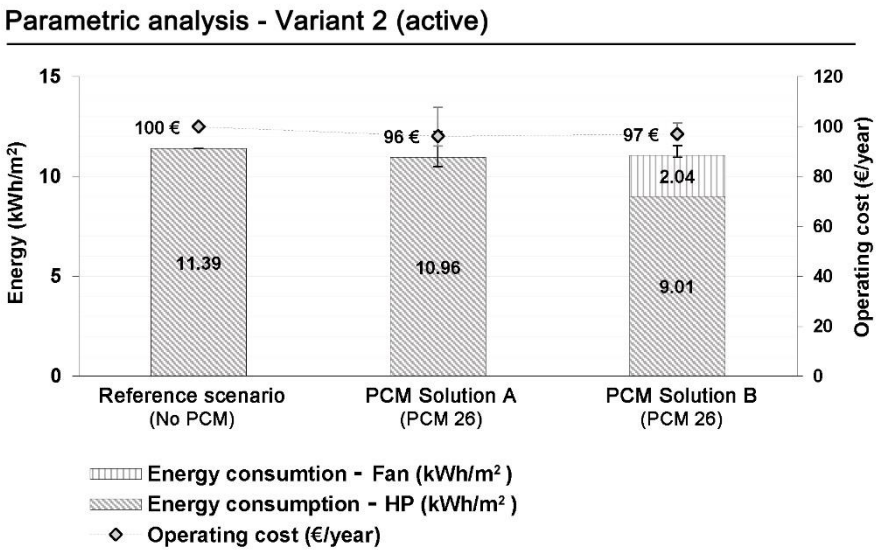

Figure 15. Results of optimised PCM-based solutions (A and B) in the case of variant 2 (active, with air-conditioning systems), compared with the reference scenario (no PCM).

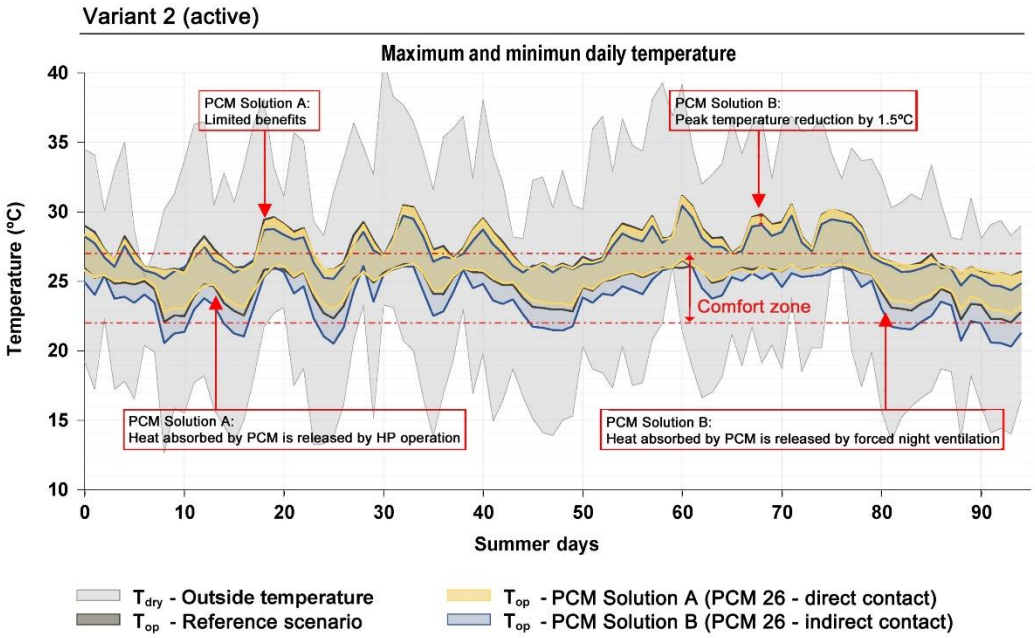

Figure 16. Maximum and minimum daily temperature of optimised PCM-based solutions (A and B) in the case of variant 2 (active, with air-conditioning systems), compared with outside temperature oscillation (T_{dry}) and the reference scenario without PCM (T_{op}).

- **PCM Solution A (direct contact) in variant 2 (active)** does not provide any environmental or economic benefits. All heat absorbed by the PCM cannot be passively released at night because of the system operation (see Fig. 16).

- **PCM Solution B (indirect contact) in variant 2 (active)** results in a reduction of energy consumption of 21% associated with the heat pump, due to the fact that the PCM is insulated from the indoor environment during HP operation, with the aim of taking advantage of night ventilation for releasing absorbed heat. However, due to the associated consumption of fan operation, the final energy consumption and associated operating costs are almost the same as the reference scenario.

However, it should be considered that peak operative temperatures, throughout daytime without HP operation, is reduced by up to 1.5 K compared to the associated reference scenario during most days of the summer (see Fig. 16).

Table 11 summarises the results of the proposed **PCM-based solutions (A and B) in variants 1 (passive) and 2 (active)**.

Table 11. Summary of results for reference scenario and optimised PCM-based solutions in two variants assessed (passive and active).

Performance indicators	Reference Scenario	PCM Solution A (direct)	PCM Solution B (indirect)
Variant 1 (passive) – free temperature oscillation			
DH (%) - T_{op} > 29ºC	38%	34% (-12%)	20% (-49%)
DH_{acm} (%)	27%	21% (-20%)	9% (-65%)
OC (€)	0 €	0 €	22 €
Variant 2 (active) –intermittent operation of AC systems			
$EC_{cooling}$ (kWh/m^2)	11.39 kWh/m^2	10.96 kWh/m^2 (-4%)	11.05 kWh/m^2 (-4%)
OC (€)	100 €	96 € (-4%)	97 € (-3%)

The results demonstrated that PCM configuration should be adjusted according to occupant requirements, climate conditions and daily cooling needs, and making general assumptions is not recommended. Following optimised configurations in passive building performance (without active systems), PCM solutions can efficiently mitigate discomfort hours by up to 65-83%. However, in the case that active air-conditioning systems are frequently required, PCM solutions should be implemented through other alternatives to enhance building performance, such as smart demand response strategies, which can provide high energy and economic savings according to recent studies [62].

4.4. Investment cost of PCM-based solutions

The current level of implementation of PCM-based solutions in buildings is quite reduced, mainly due to the fact that inappropriate solutions would lead to ineffective performance, even worsening the building performance, and also because of the high cost of phase change materials. Optimised implementation techniques through specific configurations and appropriate material section are required to achieve competitive PCM-based solutions. Fig. 17 shows a sensitivity analysis of the investment cost of the solutions studied in this work, considering a reference PCM cost of 2€/kg with a potential deviation of ±20%.

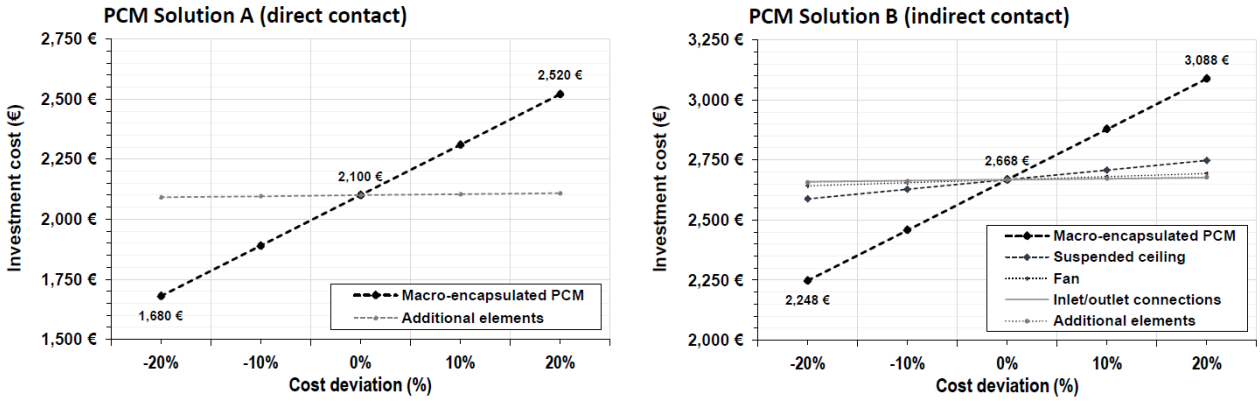

Figure 17. Sensitivity analysis of the investment cost of assessed PCM solutions (A and B).

The investment cost of **PCM solution A** ranges from 1680 € to 2520 €, and PCM solution B ranges from 2248 € to 3088 €. In both solutions, the PCM cost is higher than 75% of the whole system cost. Further research is needed to reduce material costs below 0.50 €/kg to get competitive payback periods for commercial solutions. In addition, the increase of

heat transfer rates through new heat transfer enhancement techniques, long-term stability and reliability, as well as other issues that may affect safety and feasibility, should be considered for further developments.

5. Conclusions

This paper assesses the performance of conventional and optimised PCM-based solutions for passive and low-energy cooling through parametric analysis, with the aim of identifying main design and sizing criteria for their effective implementation in buildings. The **conventional passive scenario (PCM Solution A - direct contact)** is based on a PCM layer in contact with indoor space (PCM attached at the ceiling), in which heat transfer between PCM-air is associated with natural convection, and the **optimised low-energy cooling scenario (PCM Solution B - indirect contact)** which is designed as a PCM layer insulated from indoor space (PCM integrated within the suspended ceiling), in which the air flow is regulated by a fan to enhance heat transfer between PCM and air. Both solutions are studied without, and with, the simultaneous operation of active air-conditioning (AC) systems (variant 1 and 2, respectively). The numerical simulation was carried out in TRNSYS for a Mediterranean case study as reference scenario (basis).

The results show that PCM configurations should be adjusted according to occupant requirements, climate conditions and daily cooling needs, and making general assumptions is not recommended. Melting temperatures have to be adapted to the specific application option and climate area, as its final performance is sensitive to each climate variation and internal profile. Every case must be studied in order to evaluate its real efficiency in terms of cost and energy performance. Moreover, night ventilation is emphasised as essential for the effective regeneration of the TES material at the beginning of each day.

Based on the evaluation of the proposed **PCM-based solutions (A and B) and variants 1 and 2 (passive and active)** it is possible to extract the following conclusions:

In **variant 1 (passive), with free temperature oscillation (no AC system operation)**:

- **PCM Solution A (direct contact)** presents limited benefits associated with the low value of heat transfer between PCM and air, mainly related to natural convection. The potential TES capacity of the PCM cannot be used most days because the phase change does not occur.
- **PCM Solution B (indirect contact)** overcomes previous issues. Forcing airflow through the PCM modules increases the heat transfer between PCM and air. Also, by insulating the air chamber where the PCM is located during night ventilation, lower PCM temperatures are achieved, with the PCM being regenerated on most nights. In this situation, using only passive operating schedules (variant 1 – passive), a reduction in discomfort hours of 65% with regard to the adaptive comfort model is achieved, with a minimum operation consumption. Also, it is highlighted that the discomfort period can be reduced up to 83%, through additional improvements related to better flow properties and surface characteristics, in order to enhance heat transfer between PCM and air.

In **variant 2 (active), with the intermittent operation of AC systems:**

- **PCM Solution A (direct contact)** does not provide any environmental or economic benefits. All heat absorbed by the PCM cannot be passively released, because of the system operation.
- **PCM Solution B (indirect contact)** shows better performance. It is mainly associated to the PCM layer insulated from indoor space during AC system operation, which allows the possibility of releasing heat taking advantages of night free cooling. However, due to the consumption of fan operation, final energy consumption and associated operating cost are almost similar to the reference scenario.

Future research should be considered in building typologies where continuous operating patterns of AC systems are required. In these scenarios, PCM melting temperature should be selected according to set-point temperatures with the aim of reducing the required power of the equipment, and improving its efficiency, by adjusting system operation within the high efficiency range (avoiding partial load operation and intermittent start/stop).

Acknowledgments

This work has been supported by the Spanish Ministry of Education, Culture and Sport via a scholarship for a temporary research stay at The Technical University of Munich (EST17/00105). The authors gratefully acknowledge the financial support of the Spanish Ministry of Education, Culture and Sport via a pre-doctoral contract granted to Francisco Jesús Lizana Moral (FPU14/06583); and the ClimACT Project (SOE1/P3/P0429EU) within the Interreg Sudoe Programme, funded by European Regional Development Funds. This research was also made possible due to the support of the Institute of Architecture and Building Science (IUACC) from the University of Seville, via the internationalisation grant within the VIPPI-US.

References

[1] K.T. Huang, R.L. Hwang, Future trends of residential building cooling energy and passive adaptation measures to counteract climate change: The case of Taiwan, Applied Energy. 184 (2016) 1230–1240. doi:10.1016/j.apenergy.2015.11.008.

[2] C. Spandagos, T.L. Ng, Equivalent full-load hours for assessing climate change impact on building cooling and heating energy consumption in large Asian cities, Applied Energy. 189 (2017) 352–368. doi:10.1016/j.apenergy.2016.12.039.

[3] J. Spinoni, J. V. Vogt, P. Barbosa, A. Dosio, N. McCormick, A. Bigano, et al., Changes of heating and cooling degree-days in Europe from 1981 to 2100, International Journal of Climatology. 38 (2018) e191–e208. doi:10.1002/joc.5362.

[4] N.S. Diffenbaugh, J.S. Pal, F. Giorgi, X. Gao, Heat stress intensification in the Mediterranean climate change hotspot, Geophysical Research Letters. 34 (2007) 1–6. doi:10.1029/2007GL030000.

[5] Implementing the Energy Performance of Buildings Directive (EPBD). Featuring Country Reports, ADENE, Lisbon, 2015.

[6] International Energy Agency, Energy Efficiency 2017, 2017. doi:10.1787/9789264284234-en.

[7] P. Shen, W. Braham, Y. Yi, The feasibility and importance of considering climate change impacts in building retrofit analysis, Applied Energy. 233–234 (2019) 254–270. doi:10.1016/j.apenergy.2018.10.041.

[8] S. Álvarez, L.F. Cabeza, A. Ruiz-Pardo, A. Castell, J.A. Tenorio, Building integration of PCM for natural cooling of buildings, Applied Energy. 109 (2013) 514–522. doi:10.1016/j.apenergy.2013.01.080.

[9] J. Lizana, R. Chacartegui, A. Barrios-Padura, C. Ortiz, Advanced low-carbon energy measures based on thermal energy storage in buildings: A review, Renewable and Sustainable Energy Reviews. 82 (2018) 3705–3749. doi:10.1016/j.rser.2017.10.093.

[10] J. Lizana, R. Chacartegui, A. Barrios-Padura, J.M. Valverde, C. Ortiz, Identification of best available thermal energy storage compounds for low-to-moderate temperature storage applications in buildings, Materiales de Construcción. 68 (2018) 1–35. doi:https://doi.org/10.3989/mc.2018.10517.

[11] M.A. Wahid, S.E. Hosseini, H.M. Hussen, H.J. Akeiber, S.N. Saud, A.T. Mohammad, An Overview of Phase Change Materials for Construction Architecture Thermal Management in Hot and Dry Climate Region, Applied Thermal Engineering. 112 (2017) 1240–1259. doi:10.1016/j.applthermaleng.2016.07.032.

[12] V.A.A. Raj, R. Velraj, Review on free cooling of buildings using phase change materials, Renewable and Sustainable Energy Reviews. 14 (2010) 2819–2829. doi:10.1016/j.rser.2010.07.004.

[13] K. Du, J. Calautit, Z. Wang, Y. Wu, H. Liu, A review of the applications of phase change materials in cooling, heating and power generation in different temperature ranges, Applied Energy. 220 (2018) 242–273. doi:10.1016/j.apenergy.2018.03.005.

[14] S. Ramakrishnan, X. Wang, J. Sanjayan, J. Wilson, Thermal performance of buildings integrated with phase change materials to reduce heat stress risks during extreme heatwave events, Applied Energy. 194 (2017) 410–421. doi:10.1016/j.apenergy.2016.04.084.

[15] X. Mi, R. Liu, H. Cui, S.A. Memon, F. Xing, Y. Lo, Energy and economic analysis of building integrated with PCM in different cities of China, Applied Energy. 175 (2016) 324–336. doi:10.1016/j.apenergy.2016.05.032.

[16] U. Berardi, M. Manca, The Energy Saving and Indoor Comfort Improvements with Latent Thermal Energy Storage in Building Retrofits in Canada, Energy Procedia. 111 (2017) 462–471. doi:10.1016/j.egypro.2017.03.208.

[17] X. Sun, Q. Zhang, M.A. Medina, S. Liao, Performance of a free-air cooling system for telecommunications base stations using phase change materials (PCMs): In-situ tests, Applied Energy. 147 (2015) 325–334. doi:10.1016/j.apenergy.2015.01.046.

[18] A. de Gracia, Dynamic building envelope with PCM for cooling purposes – Proof of concept, Applied Energy. 235 (2019) 1245–1253. doi:10.1016/j.apenergy.2018.11.061.

[19] T. Khadiran, M.Z. Hussein, Z. Zainal, R. Rusli, Advanced energy storage materials for building applications and their thermal performance characterization: A review, Renewable and Sustainable Energy Reviews. 57 (2016) 916–928. doi:10.1016/j.rser.2015.12.081.

[20] S. Wijesuriya, M. Brandt, P.C. Tabares-Velasco, Parametric analysis of a residential building with phase change material (PCM)-enhanced drywall, precooling, and variable electric rates in a hot and dry climate, Applied Energy. 222 (2018) 497–514. doi:10.1016/j.apenergy.2018.03.119.

[21] D. David, F. Kuznik, J.J. Roux, Numerical study of the influence of the convective heat transfer on the dynamical behaviour of a phase change material wall, Applied Thermal Engineering. 31 (2011) 3117–3124. doi:10.1016/j.applthermaleng.2011.04.001.

[22] H. Liu, H.B. Awbi, Performance of phase change material boards under natural convection, Building and Environment. 44 (2009) 1788–1793. doi:10.1016/j.buildenv.2008.12.002.

[23] Y. Cascone, A. Capozzoli, M. Perino, Optimisation analysis of PCM-enhanced opaque building envelope components for the energy retrofitting of office buildings in Mediterranean climates, Applied Energy. 211 (2018) 929–953. doi:10.1016/j.apenergy.2017.11.081.

[24] H. Weinläder, W. Körner, B. Strieder, A ventilated cooling ceiling with integrated latent heat storage - Monitoring results, Energy and Buildings. 82 (2014) 65–72. doi:10.1016/j.enbuild.2014.07.013.

[25] Y. Hu, P.K. Heiselberg, A new ventilated window with PCM heat exchanger—Performance analysis and design optimization, Energy and Buildings. 169 (2018) 185–194. doi:10.1016/j.enbuild.2018.03.060.

[26] T. Santos, C. Wines, N. Hopper, M. Kolokotroni, Analysis of operational performance of a mechanical ventilation cooling system with latent thermal energy storage, Energy and Buildings. 159 (2018) 529–541. doi:10.1016/j.enbuild.2017.11.067.

[27] Cool-phase. Natural Cooling and Low Energy Ventilation. Monodraught Ltd, (n.d.). http://www.cool-phase.net/ (accessed April 11, 2016).

[28] J.J. Lizana, M. Molina-Huelva, A. Serrano-jim, A. Serrano-Jiménez, J.J. Lizana, M. Molina-Huelva, et al., Decision-support method for profitable residential energy retrofitting based on energy-related occupant behaviour, Journal of Cleaner Production. 222 (2019) 622–632. doi:10.1016/j.jclepro.2019.03.089.

[29] Presidencia del Gobierno, Decreto 2429, de 6 de julio, por el que se aprueba la Norma Básica de la edificación NBE-CT-79, sobre Condiciones Térmicas de los Edificios, España, 1979.

[30] J. Lizana, R. Chacartegui, A. Barrios-Padura, J.M. Valverde, Advances in thermal energy storage materials and their applications towards zero energy buildings: A critical review, Applied Energy. 203 (2017) 219–239. doi:10.1016/j.apenergy.2017.06.008.

[31] C. Castellón, M. Medrano, J. Roca, M. Nogués, Use of microencapsulated phase change materials in building applications, in: Buildings X: Thermal Performance of Exterior Envelopes of Whole Buildings, ASHRAE, 2007: pp. 1–6. http://celsius.co.kr/phase_change_materials/download/energy/Use_of_Microencapsulated_PCM_in_Building_Applications.pdf.

[32] A. Oliver, F.J. Neila, A. García, Caracterización térmica de placas de yeso con material de cambio de fase incorporado, Informes de La Construcción. 62 (2010) 55–66. doi:10.3989/ic.09.036.

[33] Phase Change Materials - BASF - Micronal PCM, (n.d.). http://www.micronal.de/portal/basf/ien/dt.jsp?setCursor=1_290798 (accessed April 26, 2016).

[34] Alba balance solid plasterboards - Rigips Saint-Gobain, (n.d.). http://ch.rigips.de/download/rigips_alba_balance_infobro_en_low.pdf (accessed May 30, 2016).

[35] Knauf Comfortboard - Knauf, (n.d.). http://www.knauf.co.uk/product-range-overview/plasterboard/knauf-comfortboard (accessed May 30, 2016).

[36] Rubitherm. Phase change materials, (n.d.). http://www.rubitherm.eu/en//index.html (accessed January 15, 2016).

[37] PCM Products Limited, (n.d.). http://www.pcmproducts.net/.

[38] TRNSYS v18. A transient system simulation program, (n.d.).

[39] ASHRAE, ASHRAE Guideline 14-2014. Measurement of Energy, Demand, and Water Savings, (2014). www.ashrae.org/technology.

[40] G.R. Ruiz, C.F. Bandera, Validation of calibrated energy models: Common errors, Energies. 10 (2017). doi:10.3390/en10101587.

[41] ISO 7730:2005. Ergonomics of the thermal environment. Analytical determination and interpretation of thermal comfort using calculation of the PMV and PPD indices and local thermal comfort criteria, (2005).

[42] Condiciones de aceptación de Procedimientos alternativos a LIDER y CALENER, Instituto para la Diversificación y Ahorro de la Energía (IDAE), 2009.

[43] ISO 13790:2008. Energy performance of buildings. Calculation of energy use for space heating and cooling, (2011).

[44] J. Lizana, A. Serrano-Jimenez, C. Ortiz, J.A. Becerra, R. Chacartegui, Energy assessment method towards low-carbon energy schools, Energy. (2018). doi:10.1016/j.energy.2018.06.147.

[45] EN 13465:2004. Ventilation for buildings. Calculation methods for the determination of air flow rates in dwellings, (2004).

[46] R. Escandón, R. Suárez, J.J. Sendra, On the assessment of the energy performance and environmental behaviour of social housing stock for the adjustment between simulated and measured data: The case of mild winters in the Mediterranean climate of southern Europe, Energy and Buildings. 152 (2017) 418–433. doi:10.1016/j.enbuild.2017.07.063.

[47] EN 15242, EN 15242:2007. Ventilation for buildings. Calculation methods for the determination of air flow rates in buildings including infiltration, (2007).

[48] H. Johra, P. Heiselberg, Influence of internal thermal mass on the indoor thermal dynamics and integration of phase change materials in furniture for building energy storage: A review, Renewable and Sustainable Energy Reviews. 69 (2017) 19–32. doi:10.1016/j.rser.2016.11.145.

[49] TRNSYS 18 Technical Documentation. Volume 9: Tutorials, (n.d.).

[50] S.N. Al-Saadi, Z. Zhai, Modeling phase change materials embedded in building enclosure: A review, Renewable and Sustainable Energy Reviews. 21 (2013) 659–673. doi:10.1016/j.rser.2013.01.024.

[51] M. Saffari, A. de Gracia, S. Ushak, L.F. Cabeza, Passive cooling of buildings with phase change materials using whole-building energy simulation tools: A review, Renewable and Sustainable Energy Reviews. 80 (2017) 1239–1255. doi:10.1016/j.rser.2017.05.139.

[52] J. Lizana, D. Friedrich, R. Renaldi, R. Chacartegui, Energy flexible building through smart demand-side management and latent heat storage, Applied Energy. 230 (2018) 471–485. doi:10.1016/j.apenergy.2018.08.065.

[53] TRANSSOLAR Software | TS Nostandard TYPEs, (n.d.). http://trnsys.de/docs/komponenten/komponenten_ts_en.htm (accessed July 18, 2018).

[54] A. Dentel, W. Stephan, TRNSYS 17 TYPE 399. Phase change materials in passive and active wall constructions, (2013) 1–9. https://trnsys.de/download/de/ts_type_399_en.pdf.

[55] J. Kośny, Thermal and Energy Modeling of PCM-Enhanced Building Envelopes., in: PCM-Enhanced Building Components, Springer, Cham, 2015: pp. 167–234. doi:https://doi.org/10.1007/978-3-319-14286-9_6.

[56] G.N. Tiwari, R. Kumar Mishra, Chapter 11. Energy and Exergy Analisis, in: Advanced Renewable Energy Sources, The Royal Society of Chemistry, 2012.

[57] K. Yanbing, J. Yi, Z. Yinping, Modeling and experimental study on an innovative passive cooling system - NVP system, Energy and Buildings. 35 (2003) 417–425. doi:10.1016/S0378-7788(02)00141-X.

[58] G. Hed, R. Bellander, Mathematical modelling of PCM air heat exchanger, Energy and Buildings. 38 (2006) 82–89. doi:10.1016/j.enbuild.2005.04.002.

[59] A. Castell, I. Martorell, M. Medrano, G. Pérez, L.F. Cabeza, Experimental study of using PCM in brick constructive solutions

for passive cooling, Energy and Buildings. 42 (2010) 534–540. doi:10.1016/j.enbuild.2009.10.022.

[60] EN 15251, EN 15251:2008. Indoor environmental input parameters for design and assessment of energy performance of buildings addressing indoor air quality, thermal environment, lighting and acoustics, (2008).

[61] S. Carlucci, L. Bai, R. de Dear, L. Yang, Review of adaptive thermal comfort models in built environmental regulatory documents, Building and Environment. 137 (2018) 73–89. doi:10.1016/j.buildenv.2018.03.053.

[62] S. Farah, M. Liu, W. Saman, Numerical investigation of phase change material thermal storage for space cooling, Applied Energy. 239 (2019) 526–535. doi:10.1016/j.apenergy.2019.01.197.